

Magnetic resonance in oxygen-doped $\text{La}_2\text{NiO}_{4+\delta}$

N.J. Poirot¹, P. Simon¹, P. Odier^{1,a}, and J.M. Bassat²¹ Centre de Recherches sur la Physique des Hautes Températures, CNRS, 45071 Orléans Cedex 2, France² ICMCB, CNRS, 33608 Pessac Cedex, France

Received: 3 November 1997 / Accepted: 23 December 1997

Abstract. We report an investigation of magnetic resonance by ESR in oxygen-doped $\text{La}_2\text{NiO}_{4+\delta}$ emphasizing extensively for the first time the role of oxygen stoichiometry. The work is performed at room temperature and on powders with $0.015 \leq \delta \leq 0.17$. At low field an hysteresis is detected between increasing and decreasing fields, it depends upon δ . The resonance lines have characteristic features of ferromagnetic resonance. The intensity ($I(\Delta H_{pp})^2$) is used as an experimental parameter for investigating the effect of δ . It allows to built a diagram closely connected to the phase diagram $T - \delta$. It suggests a ferromagnetic coupling depending upon δ . When the (average) structure is tetragonal the low intensity is due to a magnetic polaron of low resistivity. In ranges where a phase separation is detected, the ferromagnetic coupling has a structural origin (DM or local anisotropy) with apparently a strong influence on the electrical resistivity.

PACS. 72.80.-r Conductivity of specific materials – 75.80.+q Magnetomechanical and magnetoelectric effects, magnetostriction – 76.50.+g Ferromagnetic, antiferromagnetic, and ferrimagnetic resonances; spin-wave resonance

Introduction

Increasing interest is devoted to $\text{Ln}_2\text{NiO}_{4+\delta}$ oxides owing to the recent discovery of new physical properties in these compounds ([1,2] and references herein). Their understanding is a key factor to shed new light on physical properties of the normal state of high T_c superconducting cuprates. At the heart of the problem is the behavior of holes in a 2D AF spin lattice and their effect on spin fluctuations. Recently, important new results concerning this problem came out in lanthanum nickelates ($\text{La}_2\text{NiO}_{4+\delta}$) where stripe correlations of spins and holes were observed, this subject is excellently reviewed in reference [1]. In this description, stripes of antiferromagnetically coupled Ni spins are separated by periodically ordered antiphase domain walls where holes are located. Stripes may be Ni or O centered, according to δ , in the latter case, the number of spins may be non-compensated evidencing local ferrimagnetic behavior [2]. Note that this structuration of charges and spins may be equally described in terms of stripes of polarons [3,4] that polarize the spin lattice in spin polarons.

Electron Spin Resonance (ESR) is ideally suited for probing coupled spins and their dynamics. Unfortunately, in-plane Cu^{2+} species have been un-observable in high- T_c compounds [5–7] until recently where EPR signals in $\text{La}_{2-x}\text{Sr}_x\text{CuO}_4$ single crystals were attributed to localized EPR active centers [8]. The linewidth of the signal shows a large enhancement below some temperature when the spin

susceptibility is depressed suggesting a strong coupling of the EPR probe to the spin fluctuations. According to the authors, the EPR probes doped p-holes that are coupled to the Cu spins in a three spin-polaron [9]. On the other hand, large and strong signals have been extensively studied in AF cuprates of T' structure [10] with the aim to understand the origin of weak ferromagnetism [10,11] in this structure and to discuss the structure of magnetically ordered Eu_2CuO_4 [12]. In oxygen-doped lanthanum nickelate ($\text{La}_2\text{NiO}_{4+\delta}$), attempts to detect EPR signals from Ni^{2+} species have been also unsuccessful [13,14] except for signals issued from Gd in Gd-doped $\text{La}_2\text{NiO}_{4+\delta}$ [13]. However a strong resonance line was reported in stoichiometric or reduced $\text{La}_{2-x}\text{Sr}_x\text{NiO}_{4-\delta}$ [15] but it could presumably originate from Ni° formed during the process or to paramagnetic species in the neighborhood of oxygen vacancies. Very broad resonance lines in electrochemically oxidized $\text{La}_2\text{NiO}_{4.25}$ [16,17] were also reported and attributed to low spin (LS) Ni^{3+} ($t_{2g}^6 d_{x^2-y^2}^1$) or alternatively to Ni^+ ($t_{2g}^6 d_{x^2-y^2}^2 d_{z^2}^1$). Three years ago, narrow and complex EPR signals were reported in Zn-doped $\text{La}_2\text{NiO}_{4+\delta}$, their envelope gets narrower upon heating and the intensity suddenly falls down above 650 K [18]. A complete view for $\text{La}_2\text{NiO}_{4+\delta}$ is nowadays lacking especially as regarding the δ -dependency.

This article is the first extensive investigation concerning ESR signals in $\text{La}_2\text{NiO}_{4+\delta}$ versus δ at room temperature. It is performed on powders equilibrated in appropriate conditions to provide $0.015 < \delta < 0.17$ and it completes preliminary investigations more focused

^a e-mail: odier@cnrs-orleans.fr

on magnetic behavior [19]. The data are analyzed by considering ferromagnetic contributions as the main ingredient of the resonance lines and discussed *vs.* δ together with structural and resistivity data performed on similar samples.

Experimental

Powders of $\text{La}_2\text{NiO}_{4+\delta}$ are formed by a modified sol-gel method described elsewhere [20,21]. All precursors were pure (> 99.99%) and one advantage of the method is the absence of crushing step. The powders just need to be gently de-agglomerated in an agate mortar before their successive heat treatments. Chemical analyses (Mg: 80 ppm; Ba, Ti, Cr, Co, Cu < 50 ppm; Zr: 150 ppm, Pr and Gd 200 ppm; other < 10 ppm) shows that only Pr or Gd might contribute. According to their shape and characteristics, the ESR signals measured here (see below) cannot be attributed to signals from paramagnetic rare earth like Gd^{3+} which is on the other hand the only rare earth susceptible to be observable at room temperature.

The powders are made of fine grains, aggregated in compacts with size ranging from $0.5 \mu\text{m}$ to $\sim 10 \mu\text{m}$ as estimated through scanning electron microscopy. Annealing in Ar/O_2 or $\text{Ar}/5\%\text{H}_2$ mixtures at different temperatures (in the range 300-500 °C) enables to adjust their oxygen stoichiometry from $\delta = 0.17$ to $\delta \approx 0$. Excess oxygen δ was deduced from the weight variation measured after total reduction of the sample to $\text{La}_2\text{O}_3 + \text{Ni}$ in a thermogravimetric apparatus (TAG 1600, Setaram Lyon, France). X-ray diffraction using the $\text{CuK}\alpha$ radiation (Ni filtered) has been used to characterize the phases of these powders.

EPR spectra are registered on a Bruker ER200D device working in X-band (9.4 GHz), with a standard TE102 cavity (some spectra were also recorded with a Q-band device). The spectra are obtained from powders inserted in pure silica tubes. Some of our compounds have a sufficiently low resistivity ($0.1 \Omega \text{ cm}$) to modify the tuning of the resonant cavity when their mass is too large. In such a case, we reduce the quantity of powdered sample in order to marginally modify the cavity tuning. The probed mass ranged then from a few mg for the most conductive samples up to 30 mg for the less conductive one. Note that in all cases, the small grain size of our powders provides a skin depth ($> 50 \mu\text{m}$) larger than the grain size ensuring a bulk origin for the reported signals. Both empty cavity and empty tubes are tested before recording the spectra for a given δ . The reproducibility of the signals is checked systematically.

Resistivities are measured on sintered ceramics (> 85–90% of the theoretical density) submitted to annealing under progressively increasing reducing conditions. The oxygen stoichiometry of the sample is measured on a small sintered part reduced in same time than the sample for resistivity. The resistivity is obtained by the four probe method between 4 and 300 K with silver painted electrodes.

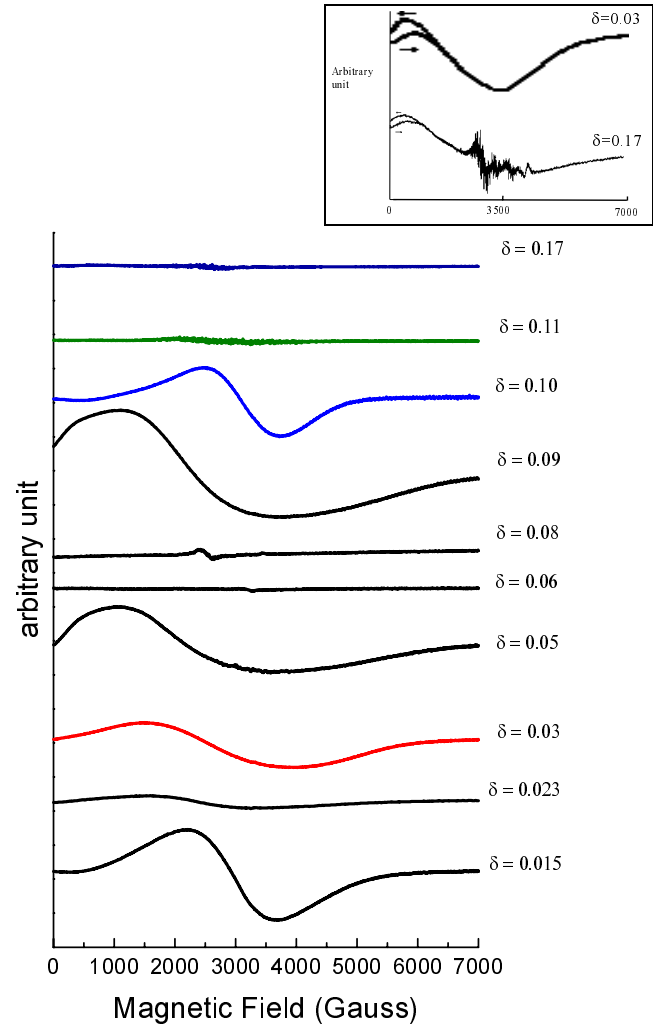


Fig. 1. ESR of $\text{La}_2\text{NiO}_{4+\delta}$ *vs.* δ measured on powders at room temperature (X-band). Vertical scale is arbitrary. Inset shows a low field hysteresis for two compositions also observed in all other samples.

Results and discussion

ESR versus δ

In a previous paper concerning $\text{Pr}_2\text{NiO}_{4+\delta}$ we have shown by infrared spectroscopy that hole doping affects essentially the in-plane properties [22]. Similar results are also observed in $\text{La}_2\text{NiO}_{4+\delta}$. Thus, oxygen stoichiometry is at first view a pertinent parameter to modify the hole density in the 2D antiferromagnetic lattice of Ln_2NiO_4 oxides. The doping mechanisms might be however complex if phase separation or charge ordering prevails. On the other hand, injected holes are expected to modify the AF coupling, this is probed here by studying magnetic absorption in an ESR spectrometer.

Figure 1 shows a general view of the resonance lines for various values of δ ranging from 0 to 0.17. In this figure, the vertical unit is arbitrary but identical for all these samples, this is allowed by the precautions explained in the experimental part. For the stoichiometric compound ($\delta = 0$)

we have been unable to detect any resonance at 300 K as expected in an ordered AF phase. This supports the Ni° origin of the resonance in the samples quoted in the introduction. For $\delta > 0$, the spectra are composed of one or two broad bands which intensity differs strongly according to δ . For example the spectra concerning $\delta = 0.05$ and 0.09 have two components also visible for $\delta = 0.08$, but with a reduced intensity and a larger separation. Conversely, only one main absorption is observed for $\delta = 0.015$ and 0.1 . For $0.06 \leq \delta \leq 0.08$ and $\delta > 0.1$, the recorded intensity falls down to a very small value and the signal become complex and composed of a multitude of very thin, fully reproducible resonance lines, not noise, shown in the inset of this figure. At low field, an hysteretic absorption is clear, it has been found in all our samples and depends upon δ . This feature traduces the existence of a ferromagnetic component also seen in the dc magnetization [23]. Note that the hysteretic cycle closes at the same field in both dc magnetization and ESR experiments. Ferromagnetic component has been already mentioned earlier in phases having low δ [24,25] but suspected to be attributable to Ni° species. In the highly oxidized $\text{La}_2\text{NiO}_{4.16}$, its presence [19] rules out Ni° contribution and emphasizes an intrinsic origin to the ferromagnetic component linked to the hole-doping itself. The resonance field of the lines increases with the frequency (experiments in Q -band) but not in a linear way, moreover the linewidth increases also with the frequency. These features are typical behavior of ferromagnetic resonance [26] and were also observed in T' cuprates [10]. The resonance width ranges from 1 to 2 kG (at 300 K), it is of the same order of magnitude for powders and thin monocrystalline slabs ($< 200 \mu\text{m}$) suggesting a minor contribution of demagnetizing effects. It is to recall that the main factor influencing magnetic properties at room temperature of this compound is antiferromagnetic fluctuations in the NiO_2 plane [27]. The dc susceptibility is effectively small ($\sim 10^{-2}$ emu/g) with a flat temperature dependence [23] (less than a factor 4 from 50 to 1200 K). The ferromagnetism probed here through the recorded resonance is a weak ferromagnetism. The strong shifts of the lines with doping (compare $\delta = 0.08$ with $\delta = 0.09$) suggests modifications of the corresponding frequency-field diagrams with δ , *i.e.*, spin gaps. Studies on crystals should be undertaken to go further on this aspect. In the absence of such data we prefer to screen over the effect of oxygen stoichiometry.

A quantitative way of comparing the spectra is to use their intensity approximated by $I(\Delta H)^2$, Figure 2. It would have been better to proceed by double integration of the spectrum but the low field absorption precludes to do this precisely. We then estimate $I(\Delta H)^2$ as follows: I is the peak-to-peak height measured for the main contribution of the line, it is normalized to the sample mass. The inflection point of the derived peak can be reasonably located on the plot, it enables to calculate the half width ($\Delta H/2$) and then the product $I(\Delta H)^2$. Our aim is to probe the δ -dependence of the absorption, not to give absolute values. Figure 2 shows strong variations of $I(\Delta H)^2$ versus δ , certainly larger than the errors of the

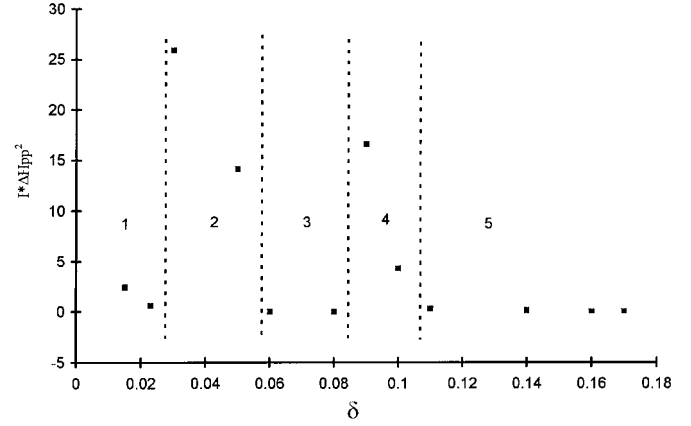


Fig. 2. ESR intensity $I\Delta H_{pp}^2$ vs. oxygen excess δ (at 300 K). ΔH_{pp} is the peak-to-peak linewidth (Gauss) and I the peak-to-peak intensity.

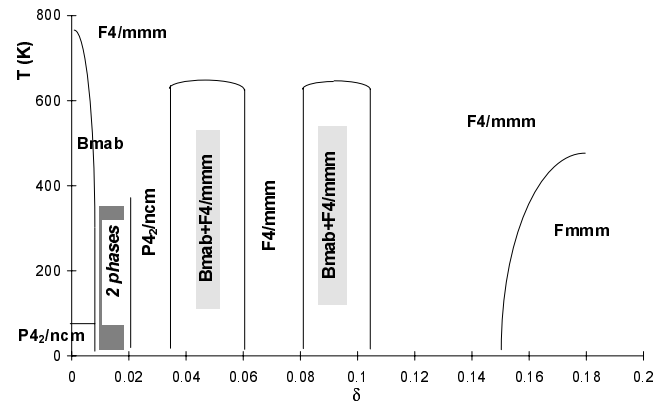


Fig. 3. Proposed phase diagram for $\text{La}_2\text{NiO}_{4+\delta}$.

procedure. Note that we have compared these absorptions with that of CuSO_4 to estimate the equivalent number of free spins that would lead to the same absorption. It is in the range of 60% of the spins assuming one spin per Ni^{2+} for the compound $\delta = 0.03$, this value falls to less than 10% when $\delta > 0.1$. The same variation is found by considering the product $I(\Delta H)^2$, Figure 2. From this figure, it appears that the data fall in 5 ranges labeled 1 to 5, delimiting areas where the ESR intensity differs substantially. We assume these variations reflects strong differences in magnetic properties with the oxygen stoichiometry. We now show the relationship with the structural phase diagram.

Phase diagram and ESR

Let us first recall the phase diagram $T-\delta$ resumed according to Figure 3. It includes data reviewed by Tranquada *et al.* [28,29] based on investigations on crushed crystals, previous measurements on powders [28,30–33] and our own results on powders. From crystal studies, Tranquada details a phase separation and ordering phenomenon occurring in the range $0.03 \leq \delta \leq 0.11$. Ordering is analyzed

in terms of staging of oxygen in interstitial oxygen layers (stade 2 and 3) in the range $0.04 \leq \delta \leq 0.11$ and charge ordering phenomena for $\delta > 0.11$. Some differences remain with determinations from powders that are generally treated at moderate temperatures (200–400 °C) under reducing mixtures of gas (Ar/H₂) while crystals are quenched from high temperature (up to 1000 °C) in the appropriate atmosphere (CO-CO₂ when small δ are needed). The difference between crystals and powders reflects a kinetic aspect or a peculiarity of the phase diagram. In powders, two phases are found in the range $0.03 < \delta < 0.1$, they are composed of an orthorhombic phase (indexed as Bmab and also called LTO phase), plus a tetragonal phase indexed as an average crystalline structure of the F4/mmm group [32,33] that we call HTT_a in the following. This later determination is considered as an average because of un-resolved broadening for several Bragg reflections. We also find these phases in our case but the precise control of δ evidences new domains reported in Figure 3. In this figure, the shaded areas denote ranges where we analyze the X-ray data according to two phases. The description in terms of two separate phases may be however not justified. In reality, in these ranges of δ , several reflections are broadened in such a way that the system can be indexed with two phases, however this might be considered as a local lowering of symmetry consecutive to an ordering phenomena. Such phenomena have been encountered recently in manganite (La,Sr)₂MnO₄ [34] where they do not correspond to a segregation of cations nor of oxygen atoms but have an electronic origin. We notice a single phase for $\delta = 0.075$ indexed in the F4/mmm SG; it was suggested by Tranquada [28], quoted as a stage 3 in the range $0.05 < \delta < 0.08$ and also announced by Yazdi [35] for $\delta \approx 0.07$ from electrochemical intercalation.

Our data concerns 300 K, however some information at low and recently high temperature [23] permits to extend the separation lines as made in Figure 3. For very low δ , the Bmab phase (LTO) transforms to P4₂/ncm (LTT) below 70 K, however Hayashi *et al.* [33] find in the range 70–300 K another LTO phase (Pccn) apparently stabilized by increasing δ . In the ranges 0.03–0.05 and 0.08–0.10, Tranquada [28] observes a phase transformation to HTT_a at around 300 K. According to our own measurements, at least on powders, the phases transform to the HTT_a structure in the range of 650 K. For larger δ , $\delta > 0.14$, a phase transition Fmmm → F4/mmm occurs which transition temperature increases with δ [31] as shown in Figure 3.

Comparing Figures 2 and 3 clearly shows that the domains marked 1 to 5 in Figure 2 nicely fit with the domains where changes in structures are observed. Except for domain 1 where the magnetic ordering ($T_N \approx 330$ K) [32] can justify a low ESR intensity, the ranges of small $I(\Delta H)^2$ are found when the structure is of high symmetry (HTT_a). In ranges 2 and 4 of strong ESR intensity, the content of phases of low symmetry is high. However, we have shown that the resonance has a marked ferromagnetic origin. This evidences then a change of the ferromagnetic properties with δ according to the phase diagram.

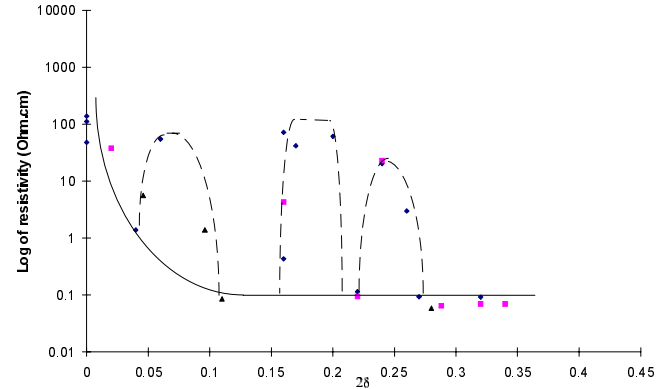


Fig. 4. Resistivity at 250 K for ceramics of various δ . The different symbols denote different samples.

Ferromagnetism in these structures has several origins. First it is a consequence of antisymmetrical superexchange coupling (Dzyaloshinski-Moriya: DM interaction [26]) which is allowed in LTT phase [24]. However weak ferromagnetism (WF) might be also present in the HTT_a phase (F4/mmm) due to local distortions as discussed in T'R₂CuO₄ phases [10–12]. On the other hand, as recalled in the introduction, holes mix with O_{2p} orbitals in a similar way to that occurring in cuprates and then favor ferromagnetic coupling between adjacent Ni spins in a double exchange interaction. This result in a so called three spin-polaron (TSP) interacting with other copper spins as demonstrated in La_{2-x}Sr_xCuO₄ [8,9]. It is interesting to note that the TSP resonance in cuprates at 300 K has a width of the same order of magnitude as in our case, suggesting a similar origin. Spin polaron has been invoked as an important ingredient of the physics of these oxides in a number of papers (see for example [36]). This polaronic magnetic coupling has not a structural origin but is essentially linked with local electronic properties (dynamical Jahn-Teller, oxygen breathing mode, apical oxygen tilts...). We then attribute the small signals of zones 3 and 5 of our ESR diagram, Figure 2, to this type of spin polaron while zones 2 & 4 are dominated by a WF of structural origin. It is interesting that the proposed spin polaron regime is found in a range where charge-spin order have been reported at low temperature [1,37]. It is also remarkable that the signals in these ranges have complex characteristics, at least on powders, being composed of a rather wide absorption line to which is superposed a multitude of very thin resonance lines. Comparisons with crystals indicates that this particular feature is a characteristic of powders.

Connection with resistivity

The resistivity *versus* δ shows also complex features [19]. Figure 4 plots data at 250 K for a set of three sintered samples which oxygen excess has been progressively reduced as said before. Using the same sample to make several successive measurements (15 for sample labeled 2) minimizes

the systematic errors made in measuring different samples. The choice of the temperature, *i.e.*, 250 K, is rather arbitrary but the thermal evolution is weakly dependent upon δ above 150 K. As it can be seen from Figure 4, a number of points has been reproduced on several samples from different powders batches. Hence the variations, that are in some cases as large as three orders of magnitude, are not due to experimental uncertainties. From this figure it is obvious that the resistivity does not decrease in proportion of the injected holes – the resistivity is not simply inversely proportional to δ – as expected in an ideal case where mobile holes would have the same concentration than the doped holes and distributed uniformly among the lattice sites. This suggests ordering phenomena and/or the existence of additional factors active on the diffusion of mobile holes. The boundaries shown in these measurements occurs precisely at the same stoichiometries than for the phase diagram, Figure 3 and ESR, Figure 2. This reflects a relationship between electronic transport and magnetic fluctuations. When the structure is highly symmetrical, we suggest the system to be driven by a magnetic polaron having a relatively low resistivity. On contrary, for the other ranges 2 and 4, where the local symmetry is low, the ferromagnetic interactions of structural origin produces a highly resistive solid by trapping the magnetic polaron or strongly diffusing it.

Although some of these arguments of this exploratory work are still qualitative, the correlation between magnetic resonance, structure and resistivity data is remarkable. It suggests to perform experiments on well established and characterized single crystals. We also notice that the organization in domains of composition alternatively insulating and conductive is not in conflict with the picture proposed by Tranquada [1] in which insulating AF domains alternate with walls where holes are concentrated. Of course we should extend this concept in a situation where it is dynamic when the temperature is above the ordering temperature. This has been actually done on a theoretical basis by Zaanen *et al.* [38].

Conclusion

Magnetic resonance has been studied in powders of $\text{La}_2\text{NiO}_{4+\delta}$. The resonance lines are broad with a low field hysteresis traducing ferromagnetic coupling. However, the intensities varies strongly with δ following the phase diagram $T - \delta$. It is complex and controlled by phase separation of electronic origin. We suggest that the differences in resonance intensity are due to different magnetic interactions. We attribute the lowest intensities, occurring when the phase is tetragonal, to spin polarons formed by a ferromagnetic coupling of nickel spins induced by O_{2p} holes. Conversely the intense signals are attributed to a ferromagnetic component having a more structural origin (local distortions or DM). We have shown a correlation with the resistivity which is low in the ranges where spin polarons are expected to predominate. All this shows a coupling between electronic transport and magnetic properties.

The authors wish to thank Dr Ph. Monod for performing SQUID measurements. We are grateful to him and Prof. Stepanov for stimulating discussions. Dr. M. Crespin is acknowledged for high T X-ray measurements.

References

1. J.M. Tranquada, *Ferroelectrics* **177**, 43-57 (1996).
2. J.M. Tranquada, P. Wochner, A.R. Moodenbaugh, D.J. Buttrey, *Phys. Rev. B* **55**, 6113 (1997).
3. C.H. Chen, S-W. Cheong, A.S. Cooper, *Phys. Rev. Lett.* **71**, 2461 (1993).
4. J. Zaanen, P.B. Littlewood, *Phys. Rev. B* **50**, 7222 (1994).
5. F. Mehran, P.W. Anderson, *Solid State Commun.* **71**, 29 (1989).
6. P. Simon, J.M. Bassat, S.B. Oseroff, Z. Fisk, S.W. Cheong, A. Wattiaux, S. Schultz, *Phys. Rev. B* **48**, 4216-4218 (1993).
7. A.Punnoose, R.J. Singh, *Int. J. Mod. Phys. B* **9**, 1123-1157 (1995).
8. J. Sichelschmidt, B. Elschner, A. Loidl, *Physica B* **230-232**, 841 (1997).
9. B.I. Kochelaev, J. Sichelschmidt, B. Elschner, W. Lemor, A. Loidl, *Phys. Rev. Lett.* **79**, 4274 (1997).
10. S.B. Oseroff, D. Rao, F. Wright, D. Vier, S. Shultz, J.P. Thompson, Z. Fisk, S-W. Cheong, M.F. Hundley, M. Tovar, *Phys. Rev. B* **41**, 1934 (1990); A. Fainstein, A. Butera, R.D. Zysler, M. Tovar, C. Rettori, D. Rao, S.B. Oseroff, Z. Fisk, S-W. Cheong, D.C. Vier, S. Schultz, *Phys. Rev. B* **48**, 16775 (1993).
11. A.A. Stepanov, P. Wyder, T. Chattopadhyay, P.J. Brown, G. Fillion, I.M. Vitebsky, A. Deville, B. Gaillard, S.N. Barilo, D.I. Zhigunov, *Phys. Rev. B.* **48**, 12979 (1993).
12. C. Rettori, S.B. Oseroff, D. Rao, J.A. Valdivia, G.E. Barberis, G.B. Martins, J. Sarrao, Z. Fisk, M. Tovar, *Phys. Rev. B* **54**, 1123 (1996).
13. F. Gervais, J.M. Bassat, P. de Rango, P. Simon, P. Odier, *Solid State Commun.* **67**, 307 (1988).
14. R. Janes, M.R. Little, M. Parker, N. Akthar, *J. Magn. Mater.* **136**, L13 (1994).
15. R.D. Sanchez, M.T. Causa, M.J. Sayagués, J.M. González-Calbet, M. Vallet-Regi, X. Obradors, *Physica B* **190**, 177 (1993).
16. A. Demourgues, A. Wattiaux, J.C. Grenier, M. Pouchard, J.L. Soubeyroux, J.M. Dance, P. Hagenmuller, *J. Solid State Chem.* **105**, 458 (1993).
17. A. Demourgues, P. Dordor, J.P. Doumerc, J.C. Grenier, E. Marquestaut, M. Pouchard, A. Villesuzanne, A. Wattiaux, *J. Solid State Chem.* **124**, 199-204 (1996).
18. P. Simon, J.M. Bassat, Y. Henrion, B. Rives, J.P. Loup, P. Odier and S.B. Oseroff, *Physica C* **235-240**, 1647 (1994).
19. N.J. Poirot, P. Odier, P. Simon, *J. Alloys and Compounds* **262-263**, 147 (1997).
20. Ch. Allançon, Thèse, Université d'Orléans, décembre 1995.
21. A. Douy, P. Odier, *Mater. Res. Bull.* **24**, 1119 (1989).
22. F. Gervais, R.P.S.M. Lobo, Ch. Allançon, N. Pellerin, J.M. Bassat, J.P. Loup, P. Odier, *Solid State Commun.* **88**, 245 (1993).
23. N.J. Poirot, thèse Université d'Orléans (décembre 1997); N.J. Poirot, Ch. Allançon, P. Odier, P. Simon, J.M. Bassat, J.P. Loup, *J. Solid State Chem.*, in press.

24. X. Battle, X. Obradors, M.J. Sayaguès, M. Vallet, J. Gonzales-Calbet, *J. Phys.: Cond. Matter* **4**, 487 (1992).
25. D.E. Rice, D.J. Buttrey, *J. Solid State Chem.* **105**, 197 (1993).
26. A. Herpin, *Théorie du magnétisme*, Bibliothèque INSTN (Paris 1968).
27. R.J. Birgeneau, G. Shirane, *Neutron Scattering Studies of Structural and Magnetic excitations in Lamellar Copper Oxides. - A Review* in *Physical Properties of High Temperature Superconductors I*, edited by D.M. Ginsberg (World Science Publ. Co. Pte. Ltd., New York, 1989) pp. 151-211.
28. J.M. Tranquada, Y. Kong, J.E. Lorenzo, D.J. Buttrey, D.E. Rice, V. Sachan, *Phys. Rev. B* **50**, 6340 (1994).
29. J.M. Tranquada, D.J. Buttrey, V. Sachan, J.E. Lorenzo, *Phys. Rev. Lett.* **73**, 1003 (1994).
30. J.D. Jorgensen, D. Dabrowski, S. Pei, D.R. Richards, D.G. Hinks, *Phys. Rev. B* **40**, 2187 (1989).
31. H. Tamura, A. Hayashi, Y. Ueda, *Physica C* **216**, 83 (1993).
32. J. Rodriguez-Carvajal, M.T. Fernandez, J.L. Martinez, *J. Phys: Condens. Matter* **3**, 3215 (1991).
33. A. Hayashi, H. Tamura, Y. Ueda, *Physica C* **216**, 77 (1993).
34. W. Bao, C.H. Chen, S.A. Carter, S.W. Cheong, *Solid State Commun.* **98**, 55 (1996).
35. I. Yazdi, S. Bhavaraju, J.F. DiCarlo, D.P. Scarfeand, A.J. Jacobson, *Chem. Mater.* **6**, 2078 (1994).
36. V. Hizhnyakov, E. Sigmund, *Physica C* **156**, 655 (1988); D.M. Frenkel, R.J. Gooding, B.I. Shraiman, E.D. Siggia, *Phys. Rev. B* **41**, 350 (1990), see also *Phase Separation in Cuprate Superconductors*, edited by E. Sigmund, K.A. Müller (Springler-Verlag, 1994) and reference [7] above.
37. J.M. Tranquada, D.J. Buttrey, V. Sachan, *Phys. Rev. B* **54**, 12318 (1996).
38. J. Zaanen, M.L. Horbach, W. van Saarloos, *Phys. Rev. B* **53**, 8671 (1996).